

# An Experimental Study of the Cooling of a Thin Glass Fiber during the Formation Process

Daxi Xiong and John H. Lienhard V

Rohsenow Heat and Mass Transfer Laboratory, MASSACHUSETTS INSTITUTE OF TECHNOLOGY  
77 Massachusetts Avenue, Room 3-162, Cambridge, MA 02139-4307 USA

## ABSTRACT

Glass fibers drawn from the melt cool primarily by convection, through a boundary layer process that has been the subject of a number of theoretical studies. In the present work, the temperature distribution along such a fiber has been measured under a range of conditions in laboratory-scale system. The measurements were made using a heated thermocouple technique, in which a thermocouple is electrically heated to a temperature near the local fiber temperature. The response of the thermocouple is observed upon slight contact with the fiber, with null response indicating temperature equality. Data were collected for diameters ranging from 20 to 50 micrometers and speeds from 1 meter per second to 6 meters per second. A comprehensive analysis was performed to estimate the uncertainty in our experiments. The analysis shows that the  $2\sigma$  uncertainty is 15.3%. Comparison between the experimental data and existing theoretical predictions shows that integral-method analyses produce the correct trends, but have systematic disagreements with the data. The direction and magnitude of these disagreements are system dependent. Potential causes may include fiber vibration, boundary layer transition, and measurement uncertainties.

To appear in: *Experimental Heat Transfer*, **17(1)**, 2004

## **1 INTRODUCTION**

Glass fibers are used to reinforce products ranging from plastics to fabrics. Such fibers are made by drawing molten glass through an array of small diameter bushings. The glass solidifies within a few centimeters of the bushing and is then pulled a distance of one to two meters prior to coating with binder compounds. Typical fiber diameters are 5 to 30  $\mu\text{m}$ , with drawing speeds varying from 15 to 90 m/s and array sizes ranging from several hundred to several thousand fibers. This process has been in use for over fifty years [1, 2].

A predictive knowledge of the cooling rate is of value in process optimization. In addition, the high tensile strength of glass fibers is sometimes attributed to the rapid cooling of the fiber while it is being formed [3]. Therefore, it is important to control the temperature profile of a drawn glass fiber.

Much research has previously been done in the area of characterizing heat transfer in forming filaments. While some of the research was experimental, a great deal of this material is theoretical in nature. An overview is presented in the following two parts of this section, one for theoretical studies and the next for experimental research. In the last part, the objectives of the present experiments are described.

### **1.1 Review of previous theoretical studies**

We consider the cooling of a single fiber as illustrated in Figure 1. Two modes of heat transfer, convection and radiation, must be examined in the fiber cooling process. From Progelhof and Throne [4] and Rea [5], if the diameter of the glass fiber is small (less than 100  $\mu\text{m}$ ), radiative cooling is very small compared with convective cooling and can be

ignored. A variety of approaches to estimating the convective heat transfer coefficient have been used in previous theoretical studies.

Glauert and Lighthill [6] assumed that the momentum boundary layer developed along a stationary, infinitely long cylinder in a moving fluid. They derived the skin friction, boundary-layer displacement, and momentum defect using a series solution of the von Karman-Pohlhausen boundary-layer integral. Although they did not consider heat transfer, their application of the von Karman-Pohlhausen technique, and their use of the nondimensional coordinate  $v_x/Va^2$  (for  $\nu$  the kinematic viscosity of air and other terms as in Figure 1), was widely adopted in the later studies.

Sakiadis [7, 8, 9] also used the boundary-layer integral technique, but he applied a different velocity profile so as to match the momentum boundary conditions in his problem. Unlike Glauert and Lighthill, Sakiadis assumed that the boundary layer developed from the point where an infinitely long cylinder issued from a wall into a surrounding medium at rest. Sakiadis considered both laminar and turbulent boundary layers, although he concluded that his model for the velocity profile in turbulent flow could not accurately predict real turbulent boundary layer flow.

Glicksman [10] employed a Reynolds analogy based on the work of Glauert and Lighthill to estimate the value of the local convective heat transfer coefficient as

$$Nu_x = \frac{4.3}{\ln\left(\frac{4\nu x}{Va^2}\right)} - \frac{12.9}{\left[\ln\left(\frac{4\nu x}{Va^2}\right)\right]^3} \quad (1)$$

The Reynolds analogy used took the air Prandtl number to be unity and thus required that the thickness of the momentum and thermal boundary layer surrounding the glass fiber be

equal. Glicksman derived the cooling time for the fibers and compared it with other theories and experimental data.

Bourne and Elliston [11] and later Bourne and Dixon [12] used the same von Karman-Pohlhausen technique to study the development of the momentum and thermal boundary layers of a constant diameter fiber. Their formulation introduced a correction factor for Prandtl number less than unity. They found that their predicted Nusselt was less than the experimental data available by 2% to 8%, depending on the axial location along the fiber.

The approach of Bourne and Dixon was extended by Sweetland and Lienhard [1] to include the effects of the water sprays that are often used to accelerate fiber cooling.

Sayles [13, 14], who cited the work of Moore and Pearson [15], introduced a formulation that took account of the boundary-layer curvature (characterized by  $1/a$ ) and showed that curvature may increase the Nusselt number by as much as 28%. Sayles estimated the convective heat transfer coefficient by resorting to the Reynolds analogy.

Beese and Gersten [16] also examined the effect of curvature. They used an asymptotic expansion with respect to the perturbation parameter

$$\varepsilon = 1/\sqrt{\text{Re}_a} \quad (2)$$

where  $\text{Re}_a = V a/\nu$ , and they developed this expression for the local Nusselt number

$$\frac{Nu_x}{\text{Re}_x} = \frac{0.349}{\sqrt{\text{Re}_x}} + \frac{0.366}{\text{Re}_a} + \frac{\theta'_{23}(x,0,0.7)}{\text{Re}_a \sqrt{x}} \quad (3)$$

where the complicated function  $\theta'_{23}$  is defined in their paper.

## 1.2 Review of previous experimental studies

Compared with the large volume of theoretical studies of fiber cooling, little experimental investigation has been published. One reason is that it is difficult to measure the temperature of a sufficiently thin, moving cylinder.

Kase and Matsuo [17] provided the generally accepted correlation for a *stationary* thin cylinder parallel to the airflow:

$$Nu_a = 0.42(Re_a)^{0.344} \quad (4)$$

Kase and Matsuo developed their correlation from data they obtained by placing a 0.2 mm diameter heated wire in an airflow parallel to the axis of the wire for values of  $Re_a$  in the range of 0.5-50. Later, Kase and Matsuo [18] extended their results to represent the presence of the cross flow more accurately.

Morris et al. [19,20] also developed a correlation for the local heat transfer coefficient by measuring the heat loss from a heated platinum filament at rest in moving air. The data were collected for 5 different filament diameters from 25.4 to 76  $\mu\text{m}$  over a temperature range from 400 K to 1100 K. They estimated the error of the correlation as 11.5% [20].

Alderson, Caress and Sager [21] performed experiments on moving glass fibers and found that, within a quite substantial distance from the orifice,  $\log[T_s(x)-T_\infty]$  decreases almost linearly with the position along the direction of motion, suggesting a constant heat transfer coefficient.

Arridge and Prior [22] measured the cooling rates of fibers 10 to 50  $\mu\text{m}$  diameter. They found that the cooling time is about 30 times slower than the theoretical prediction of Anderson [23].

Maddison and McMillan [24] measured the cooling time of thicker glass fibers (100-200  $\mu\text{m}$ ) and found that the cooling time was proportional to (velocity) $^{-0.7}$  and (radius) $^{1.5}$  and was typically on the order of seconds.

The collected data of the three papers on moving fibers are shown in nondimensional coordinates in Figure 2. The data are compared to some of the previously mentioned theoretical results and correlations [10, 12, 16, 17]. We see that, while the cooling time that some models predict is of the same order as the experimental results, there are significant differences among them. Moreover, the different groups of data disagree, suggesting either a dependence on additional variables or inaccuracies in the measurements. The general departure of the data from the laminar theory of Bourne and Dixon [12] at  $xv/Vd^2 \approx 1600$  is suggestive of a turbulent transition or some other change in the cooling mechanism in that vicinity.

### **1.3 The present experiments**

In present study, a system was set up to measure the fiber glass temperature distribution for different drawing speeds and different fiber diameters. The fibers were produced directly from molten glass in a range of sizes characteristic of manufacturing practice.

The measurement of glass fiber temperature involves a choice between two fundamentally different approaches: contact methods, such as thermocouple techniques, and non-contact methods, such as the thermal-imaging techniques. Both methods can measure the temperature of a large-sized body accurately, but neither easily allows accurate measurement of small body temperatures. In the case of the thermocouple method, for example, because the glass fiber may be small relative to the thermocouple,

the heat capacitance of the thermocouple junction may be large enough to change the fiber's temperature upon contact. Thus, the measured temperature may not be the correct temperature of the glass fiber. On the other hand, for non-contact methods such as optical pyrometry, the size of typical reinforcing fibers ( $\sim 10 \mu\text{m}$  diameter) is often smaller than the spatial resolution of the optical system within the wavelength range of interest. Therefore, background signals may be large compared to the effective thermal radiation signal. Larger fibers, such as optical fibers, have been measured optically [25].

To overcome the above-stated problems in measuring the glass fiber temperature, a heated thermocouple technique [26, 27] has been adopted for the present experiments. The heated thermocouple technique is a null technique in which a thermocouple's measuring junction is heated to some desired temperature. When this temperature matches that of the glass fiber, the thermocouple temperature does not change when the junction makes a light contact with the fiber. Compared to regular [unheated] thermocouple measurements, this method has the advantage that it can measure the temperature of a small object with minimal error due to the sensor's heat capacitance [26, 28]. Arridge [22] and Maddison [24] also adopted this method in their experiments and concluded that the heated thermocouple method technique accurately measures a thin filament's temperature; however, they did not attempt to quantify measurement uncertainties.

## **2. EXPERIMENTAL APPARATUS**

The experimental apparatus is shown schematically in Figure 3. The glass fibers studied were produced using a laboratory-scale glass melter. Glass marbles were melted in a platinum-iridium alloy crucible (or "bushing") encased in refractory cement. An array of nine small orifices was located at the bottom of the crucible, and fibers were produced by

drawing the molten glass through these orifices. The crucible was electrically heated using current drawn from a 24 kVA transformer with a 480 VAC primary side; the crucible received the secondary current of roughly 60 A at 0.78 V. The transformer was controlled by a thyristor and TCS Bushing Controller, the latter receiving feedback from a Type R thermocouple embedded in the crucible wall. The power was regulated so as to maintain a glass temperature of 1232°C (2250°F) within the crucible. The glass was a standard composition of E-glass, such as is commonly used for reinforcing fibers [29].

The fiber forming process involves a combination of extrusion and pultrusion of molten glass: the glass is pulled through the orifices by a take-up reel as well as being pushed through by the hydrostatic pressure of the molten glass above the bushing. After passing through the orifice, the molten glass necks until it solidifies at a final diameter of 20-50  $\mu\text{m}$ , depending upon the drawing speed, glass temperature, and other variables. Solidification takes place within about 1 cm of the orifice. The pressure above the molten glass was regulated so as to maintain a fixed hydrostatic pressure above the orifices. The glass fibers were pulled downward and collected on a computer controlled, motorized winder drum. These systems ensured that the fiber diameter did not vary during each experiment [30].

The fiber temperature measurement system consists of three subsystems: a thermocouple heating subsystem, a measurement subsystem, and a traversing subsystem.

The thermocouple heating subsystem includes an electrical heater, an adjustable electrical resistance, an adjustable voltage source, and an ammeter (see Figure 4). The heater is a Ni-Cr thin plate, which is installed on the tip of a three-fixed-cylinder bracket. The Ni-Cr plate is wired with copper leads, which pass through the two outer cylinders and



are connected to the power source to create a circuit. The thermocouple junction is affixed by cement on the surface of the plate. It is electrically insulated from the heater by thin layer of high-temperature-rated cement. Different temperatures at the thermocouple junction were obtained by adjusting the supplied current.

The measurement subsystem includes a Type K thermocouple, a thermocouple board, and a computer. The thermocouple wire was 50  $\mu\text{m}$  in diameter; it has a calibration uncertainty of  $\pm 6$  K in our temperature range. A National Instruments 4350 DAQ board, having a precision of  $\pm 2$  K was used to convert the thermocouple voltage to temperatures.

The heating system and the measuring system were fixed together into a single probe that was mounted in a three-dimensional traverse. The temperatures at different locations along the glass fiber were measured by traversing the probe.

### **3. MEASUREMENT TECHNIQUE**

Before discussing measurement techniques, we show the response of a heated thermocouple upon contact with a fiber. The junction temperature will respond in one of three ways when the thermocouple briefly contacts the fiber, as illustrated by the data in Figure 5:

- (i) An upward peak is observed when the fiber is contacted at a time of around 22 seconds in Figure 5. This means the temperature of the thermocouple is lower than that of the fiber. Upon contact, the fiber transfers heat to the thermocouple, raising its temperature.

(ii) No obvious change occurs in the thermocouple temperature at a time of about 45 seconds. This means the temperature of the probe is very close to the temperature of the fiber. Little heat is exchanged between them.

(iii) A downward peak is observed when contact occurs at a time of about 70 seconds in Figure 5. This means the temperature of the thermocouple is higher than that of the fiber. The temperature of the thermocouple decreases upon contact.

By seeking the condition illustrated in case (ii), measurements can be made using either a steady state or a transient probe temperature.

### **3.1 The steady state measurement technique**

In the steady state measurement method, the thermocouple probe is brought to a steady temperature before contact is made with the fiber. In this procedure, an estimated temperature is set, and then the thermocouple is permitted to contact the object. One of the above-mentioned types of response occurs. If type (i) happens, we increase the current of the circuit to increase the junction temperature. If type (iii) happens, we decrease the current to reduce the junction temperature. When type (ii) happens, the temperature of the glass fiber is obtained. Under conditions (i) & (iii), after adjusting the current to obtain another steady temperature, we make contact again. This loop will be repeated until type (ii) response is obtained.

The advantage of this method is that we can adjust the probe to any preferred temperature. This approach was used for all of our experiments.

### **3.2 Transient measurement technique**

In the transient measurement method, contact is made while the thermocouple is cooling (see Figure 6). In this procedure, the thermocouple temperature is first raised to a temperature that is somewhat higher than that estimated for the fiber. Then the heating current is reduced or cut off, causing the probe temperature drop slowly. During the cool-down, the thermocouple is repeatedly put in contact with the fiber. If contact is repeatedly broken and reestablished, a temperature profile like in Figure 6 will be recorded.

The figure shows that the temperature peak is downward during the initial contacts; this means that the probe temperature is higher than that of the fiber. Following that, no temperature peak is observed during contact, which means the thermocouple temperature approximates the temperature of the fiber. Subsequently, upward temperature peaks are found, indicating that the probe temperature is lower than the temperature of the fiber. Thus, the temperature of the fiber can be read from Figure 6. The advantage of this method is that the fiber temperature can be obtained rapidly. However, its accuracy is obviously very sensitive to the frequency of contact. We did not adopt this approach in the current experiments.

## **4. EXPERIMENTAL RESULTS**

Axial temperature profiles were measured along fibers of different diameters at different drawing speeds. Measurements began just below the orifice and continued over the next 10 to 15 cm. Care was taken to avoid radiant heating of the probe by the bushing.

The data are shown in dimensional coordinates in Figure 7. Each frame includes temperature profiles for several diameters of fiber at a single drawing speed. The graphs

cover drawing speeds ranging from 1.76 m/s to 6.15 m/s, with diameters ranging from 20  $\mu\text{m}$  to 50  $\mu\text{m}$ .

These graphs show that fiber temperature drops very quickly at first. The temperature changes from 1270 K at the orifice to 700 K or less within a 10-cm distance. After that, the cooling rate is slower. At higher drawing speeds, the fibers cool more quickly; at higher diameters, the fibers cool more slowly.

The laminar convective cooling theory [1,12] suggests that a proper nondimensionalization of the data is to plot  $(T - T_{\text{air}})/(T_0 - T_{\text{air}})$  against  $(v_x/Va^2)$ , where  $T_0$  is the [extrapolated] temperature of the glass at the outlet of the bushing. The data are shown in this form in Figure 8, together with the theoretical prediction of the temperature. Our data are close to the laminar theory, but generally somewhat below it. This indicates that the actual cooling rate of the fibers is higher than laminar convection alone will provide. Potential causes of this disagreement include laminar-to-turbulent transition (the onset of which is not understood for axially moving fibers), transverse fiber vibration (which is observed to occur most fiber drawing processes, including ours), and measurement uncertainties. We discuss the latter in the next section.

Our data are compared to past data sets and correlations in Figure 9.

## **5. MEASUREMENT UNCERTAINTIES**

The heated thermocouple technique involves several potential sources of measurement error. Among these are errors due to temperature change upon contact with the moving fiber and errors related to temperature fluctuation in the heated probe [31]. In addition, the

probe has the usual thermocouple calibration and reading uncertainties, as mentioned in Section 2.

When the heated probe sits in still air at room temperature, its reading is observed to fluctuate. At a probe temperature of 678 K (in air at 300 K), the rms fluctuation was measured to be  $\pm 16.5$  K. While this fluctuation is presumably lower when the probe is situated in the warmer air of the fiber boundary layer, for purposes of measurement we have assumed that if the temperature change of the probe is less than 16.5 K before and after contacting the fiber, the temperature of the probe equals the temperature of the fiber. Thus, all readings taken have at least this level of uncertainty.

A second uncertainty relates to convective cooling of the probe when it enters the moving air adjacent to the fiber. In still air, natural convection removes heat from the probe; in the moving air of the boundary layer, forced convection occurs. An upper bound estimate for the change in probe temperature due to the higher heat transfer coefficient of forced convection is 9.8 K [31]. The effect on fiber temperature of the changed convection condition where the probe contacts it is very small, since the fiber is moving rapidly past the probe.

Heat is conducted between the fiber and the probe during contact if their temperatures are not equal. This effect may alter the fiber temperature locally. If we assume a contact area equal to the thermocouple bead cross-section (a substantial overestimate) and a maximum *unnoticed* fiber-to-probe temperature difference of 30 K, simple estimates show the fiber temperature to change by less than 3.4 K.

Frictional heating during contact of the probe with the fiber is the remaining uncertainty. To quantify this source of error, we supported the probe on a force-measuring transducer having a 0.01 N resolution. We then took multiple measurements of the contact

force when the probe touched the fiber, giving an average value of 0.038 N. The coefficient of sliding friction for metal on glass is roughly 0.25. At a fiber speed of 5.27 m/s and a 0.2 second contact time, we find that 0.01 J is generated by friction. If half of this heat enters the moving fiber, its temperature will rise by 2 K. If the other half is taken up by the probe, its temperature rise can be estimated, allowing for convective removal of some of this heat from the probe wires. On a lower bound basis (using a transient conduction model), we find an 8.0 K change in probe temperature; on an upper bound basis (using a steady conduction model), we find a 37 K change. We take the average of these, 22 K, as the estimated frictional heating error, although we believe that the transient model is closer to the actual error.

The rms total of all uncertainties at a  $1\sigma$  level is  $\pm 30.7$  K. The relative error, based on a typical fiber-to-air temperature of difference 400 K, is 15.3% at 95% confidence ( $2\sigma$  level). This uncertainty is represented with bars around the data points in Figure 8.

## **6. CONCLUSIONS**

A heated thermocouple technique was used to measure the axial temperature profile of thin glass fibers that were drawn from a melt. The temperature profiles were obtained for a range of drawing speeds and fiber diameters. An error analysis shows that the uncertainty of the fiber-to-air temperature difference is 15.3% (at a 95% confidence level). The main uncertainty is due to frictional heating of the thermocouple probe.

The experimental data were compared to predictions in the literature that are based on the laminar Karman-Pohlhausen integral technique. The comparison between the data and the theoretical prediction shows that the integral method produces the correct trends, but that those results are systematically higher than the data. Similar disagreements with theory

are found in other data sets from the literature. The direction and magnitude of these disagreements are system dependent. Potential causes may include transverse vibration of the fibers, laminar-to-turbulent transition in the fiber boundary layer, and measurement uncertainties.

## **ACKNOWLEDGMENTS**

PPG Industries, Inc. partially sponsored this work. Portions of this work were presented at the 2001 ASME National Heat Transfer Conference.

## NOMENCLATURE

$a$	glass fiber radius (m)
$d$	glass fiber diameter (m)
$h$	convection coefficient ( $W/m^2K$ )
$k$	thermal conductivity of air ( $W/m-K$ )
$Nu_x$	local Nusselt number based on distance $x$ ( $hx/k$ )
$Nu_a$	Nusselt number based on fiber radius ( $ha/k$ )
$Re_x$	Reynolds number based on distance $x$ ( $Vx/v$ )
$Re_a$	Reynolds number based on fiber radius ( $Va/v$ )
$T$	temperature (K)
$T_{air}$	air temperature (K)
$T_O$	fiber temperature at the outlet of the orifice (K)
$T_s$	fiber surface temperature (K)
$T_\infty$	environmental temperature (K)
$V$	fiber drawing speed (m/s)
$x$	distance from the orifice of the bushing (m)
$\varepsilon$	perturbation parameter
$\nu$	viscosity ( $m/s^2$ )



## REFERENCES

1. M. Sweetland and J.H. Lienhard V, Evaporative Cooling of Continuously Drawn Fibers by Water Sprays, *Intl. J. Heat Mass Transfer*, vol.43, p.777, 2000.
2. K. L. Loewenstein, *The Manufacturing Technology of Continuous Glass Fibers*, 3<sup>rd</sup> ed., Elsevier Science Publishers B. V., Amsterdam, 1993.
3. S. Bateson, Critical Study of the Optical and Mechanical Properties of Glass Fiber, *J. Appl. Phys.*, Vol.29, No.1, p.13, 1958.
4. R. C. Progelhof and J. L. Throne, Comment on "Heat Transfer through the Axially Systematic Boundary Layer on a Moving Circular Fiber, *Intl. J. Heat Mass Transfer*, Vol.14, p.2166, 1971.
5. Samuel N. Rea, Rapid Method for Determining Concentric Cylinder Radiation View Factors, *AIAA J.*, Vol.13, No.8, p.1122, 1975.
6. M. B. Glauert and M. J. Lighthill, The Axisymmetric Boundary Layer on a Long Thin Cylinder, *Proc. Royal Soc., Series A*, p.188, 1955.
7. B. C. Sakiadis, Boundary-Layer Behavior on Continuous Solid Surfaces: I. Boundary-Layer Equations for Two-Dimensional and Axisymmetric Flow, *AIChE J.*, Vol.7, No.1, p.26, 1961.
8. B. C. Sakiadis, Boundary-Layer Behavior on Continuous Solid Surfaces: II. The Boundary Layer on a Continuous Flat Surface, *AIChE J.*, Vol.7, No.2, p.221, 1961.
9. B. C. Sakiadis, Boundary-Layer Behavior on Continuous Solid Surfaces: III. The Boundary Layer on a Continuous Cylindrical Surface, *AIChE J.*, Vol.7, No.3, p.467, 1961.

10. L. R. Glicksman, The Cooling of Glass Fibres, *Glass Technology*, Vol.9, No.5, p.131, 1968.
11. D. E. Bourne and D. G. Elliston, Heat Transfer through the Axially Symmetric Boundary Layer on a Moving Circular Fibre, *Intl. J. Heat Mass Transfer*, Vol.13, p.583, 1970.
12. D. E. Bourne and H. Dixon, The Cooling of Fibres in the Formation Process, *Intl. J. Heat Mass Transfer*, Vol.24, p.1323, 1971.
13. R. E. Sayles, A Local Similarity Solution for the Viscous Boundary Layer Flow Longitudinal to a Cylinder, *AIAA J.*, Vol.22, p.717, 1984.
14. R. E. Sayles, Approximate Solution for the Viscous Boundary layer on a Continuous Cylinder, *AIAA J.*, Vol.36, No.12, p.1917, 1990.
15. C. Moore and J. R. A. Pearson, Experimental Investigation into an Isothermal Spinning Threadline: Extensional Rheology of a Separan AP 30 Solution in Glycerol and Water, *Rheologica Acta*, Vol.14, No.5, p.153, 1975.
16. E. Beese and K. Gersten, Skin Friction and Heat Transfer on a Circular Cylinder Moving in a Fluid at Rest, *J. Applied Math. Physics*, Vol.30, p.117, 1979.
17. S. Kase and T. Matsuo, Theoretical Analysis of Melting Spinning, *J. Text. Mach. Soc. Japan*, Vol.18, No.3, p.188, 1965.
18. S. Kase and T. Matsuo, Studies on Melt Spinning. I. Fundamental Equation on the Dynamics of Melting Spinning, *J. Polymer Sci., Part A*, Vol.3, p.2541, 1965.
19. G. J. Morris, J. L. Loth, and R. E. Bond, *Cooling Rate of a Filament*, Final Contract Report to PPG Industries, Inc., 1997.
20. G. J. Morris, J. L. Loth, R. E. Bond and A. J. Cragg, *Cooling Rate of a Drawn Glass Filament*, Final Contract Report to PPG Industries, Inc., 1999.

21. J. V. Anderson, J. B. Caress and R. L. Sager, *The Cooling Rate of a Glass Fiber in the Continuous Filament Process*, Laboratory Report No. L.R.235 of Pilkington Bros. Ltd., Lathom, Lancashire, 1968.
22. R. G. C. Arridge and K. Prior, Cooling Time of Silica Fibers, *Nature*, Vol.203, p.386, 1964.
23. O. L. Anderson, Cooling Time of the Strong Glass Fibers, *J. Appl. Phys.*, Vol.29, No.1, p.9, 1958.
24. R. Maddison and P. W. McMillan, Cooling Rates of Glass Fibers, *Glass Technology*, Vol.19, No.5, p.127, 1978.
25. P. G. Simpkins and P. A. Blythe, Laws for Fiber Temperature Prediction during Drawing, *J. Heat Transfer*, Vol.199, p.652, 1997.
26. N. Sasaki, A New Method for Surface-Temperature Measurement, *Rev. Sci. Instr.*, Vol.21, No.1, p.1, 1950.
27. N. Sasaki and A. Kamada, A Recording Device for Surface Temperature Measurements, *Rev. Sci. Instr.*, Vol.23, No.6, p.261, 1952.
28. M. F. Culpin and D. M. Jones, Measurement of the Temperature of a Running Threadline, *J. Sci. Instr.*, Vol.36, p.28, 1959.
29. B. M. McKeone, *Measurement of Air Temperature and Velocities in the Fiber Glass Forming Environment*, S. M. Thesis, Massachusetts Institute of Technology, Cambridge, Massachusetts, 1999.
30. C. R. Ansbergs, *Optimization of the Glass Fiber Forming Process for Single-Tip and Small-Number-Tip Position*, S.M. Thesis, Massachusetts Institute of Technology, Cambridge, Massachusetts, 1999.

31. D. X. Xiong, *An Experimental and Theoretical Study of the Cooling of a Thin Glass Fiber during the Formation Process*, Ph.D. Thesis, Massachusetts Institute of Technology, Cambridge, Massachusetts, 2002.

## LIST OF FIGURES

Figure 1. Fiber drawn steadily downwards through an orifice.

Figure 2. Comparison of past experimental data and prediction curves.

Figure 3. Sketch of temperature measurement system for glass fiber.

Figure 4. Cross-section of heating subsystem.

Figure 5. Temperature response when a probe at an initially steady temperature contacts an object at three different temperatures.

Figure 6. Transient temperature profile with repeated contacts. The actual temperature was 331 K.

Figure 7. Temperature profiles under different drawing speeds and fiber diameters.

Figure 8. Comparison of our data to the integral-method prediction based on references [1,12]. Uncertainty bars are shown for each data point.

Figure 9. Comparison of past and present experimental data and predictions.

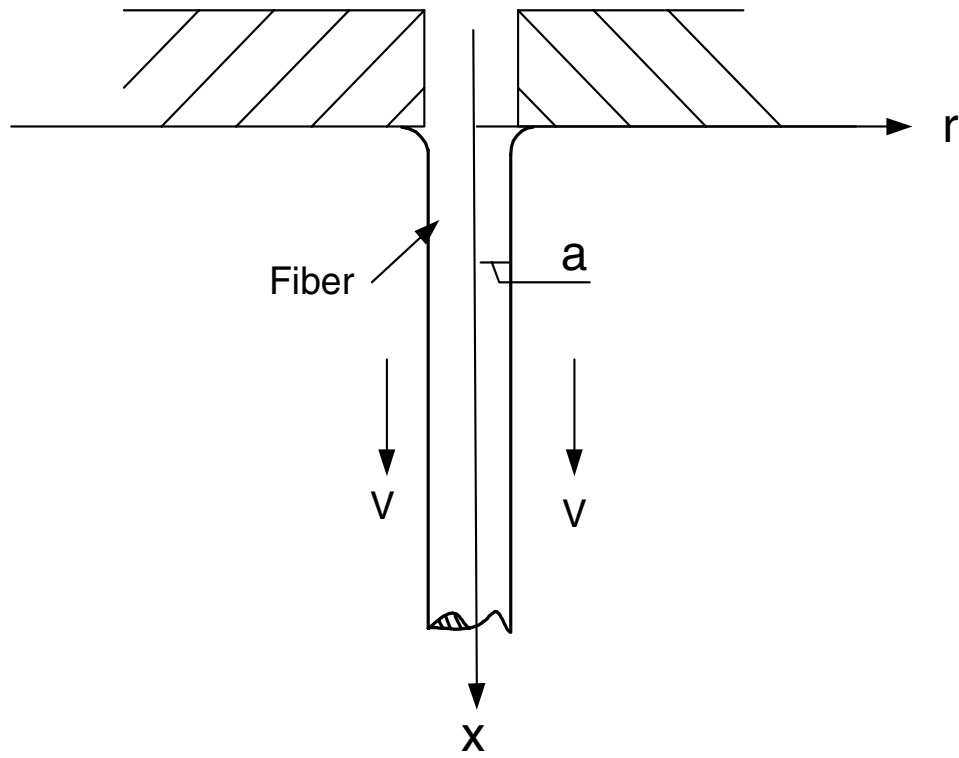


Figure 1. Fiber drawn steadily downwards through an orifice.

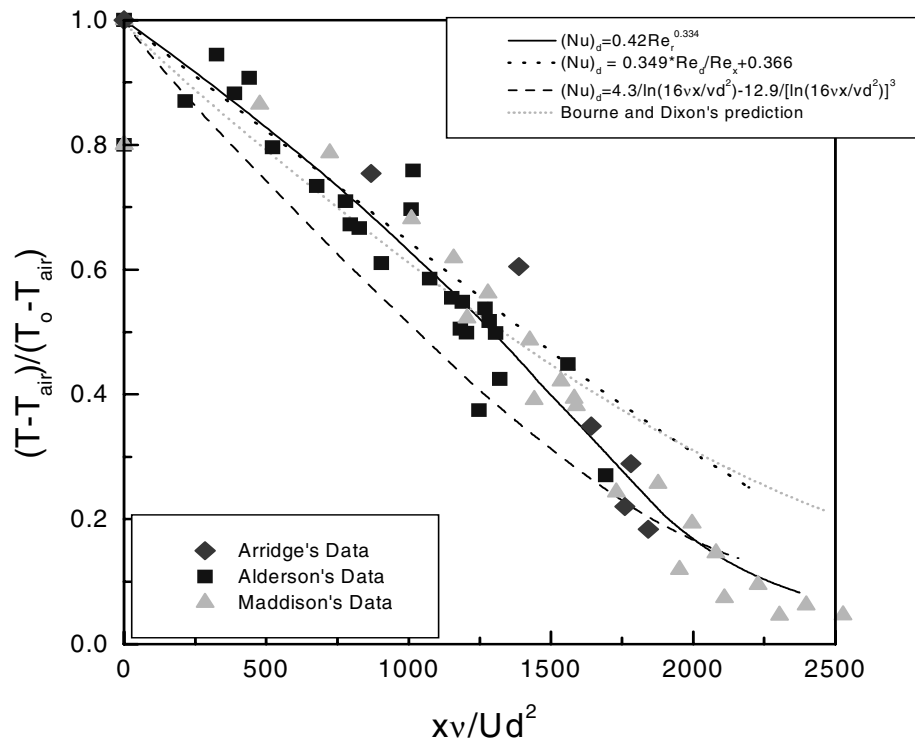


Figure 2. Comparison of past experimental data and prediction curves.

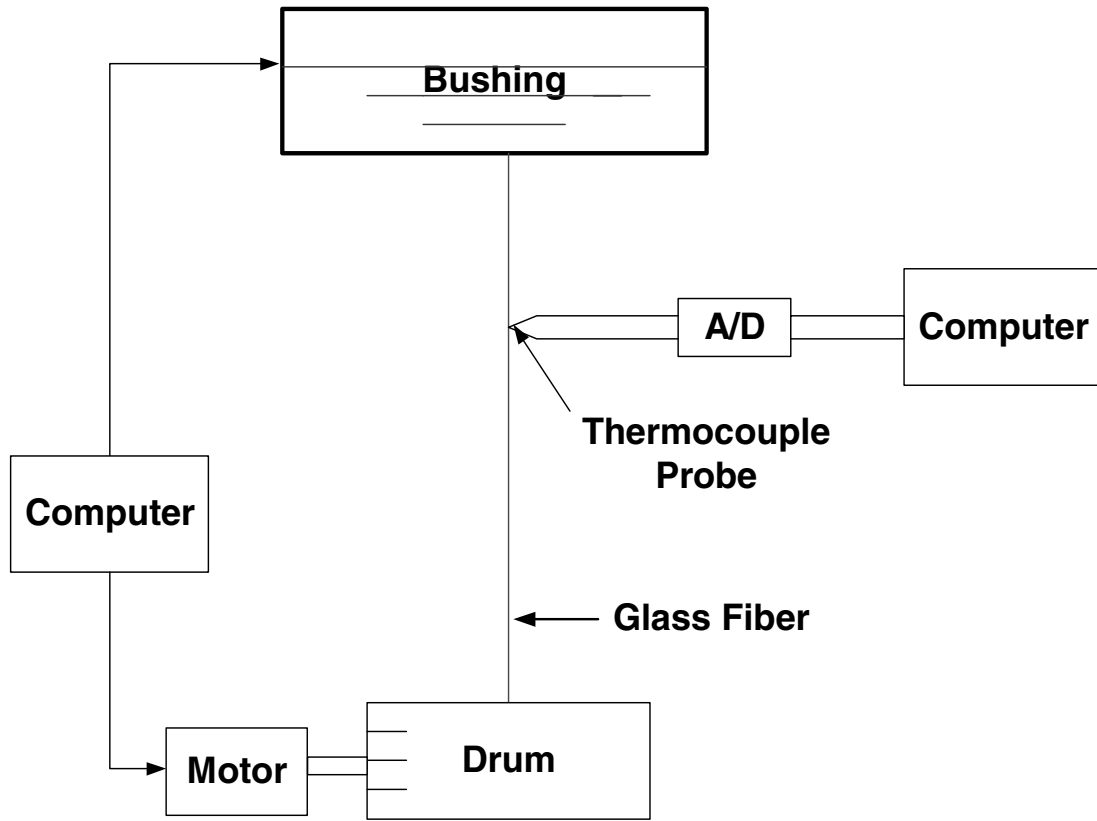


Figure 3. Sketch of temperature measurement system for glass fiber.



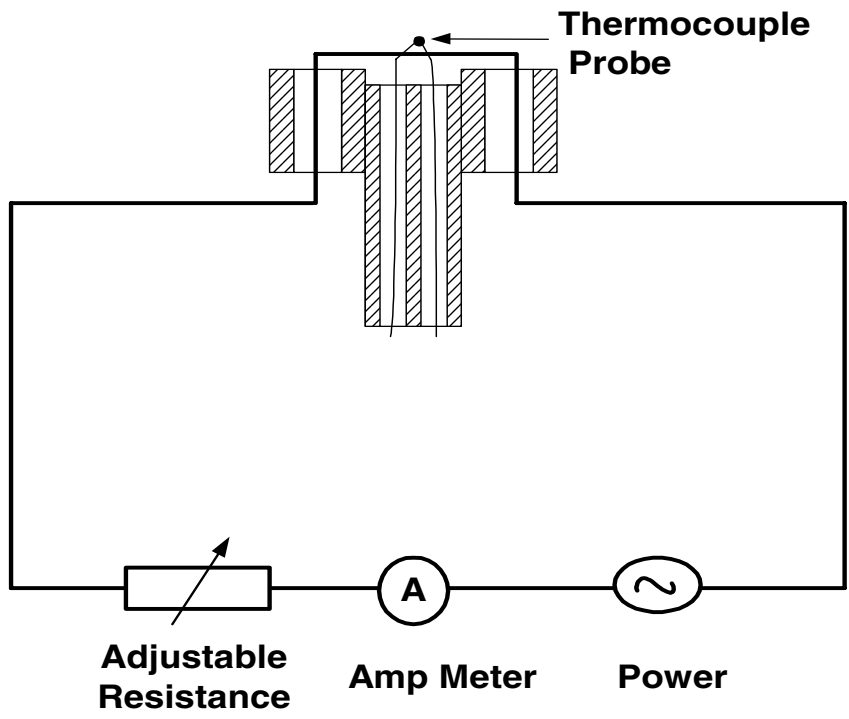


Figure 4. Cross-section of heating subsystem.

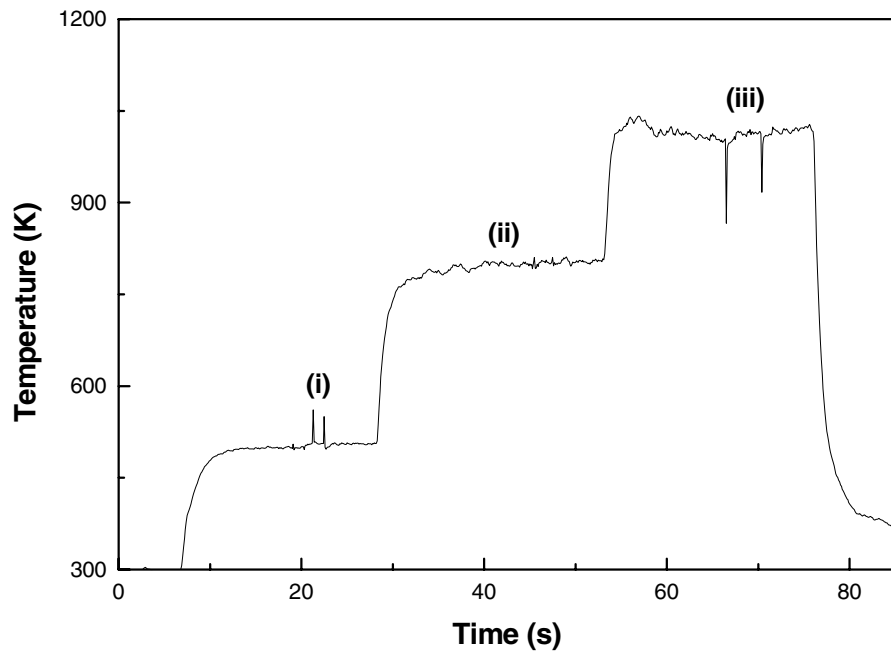


Figure 5. Temperature response when a probe at an initially steady temperature contacts an object at three different temperatures.

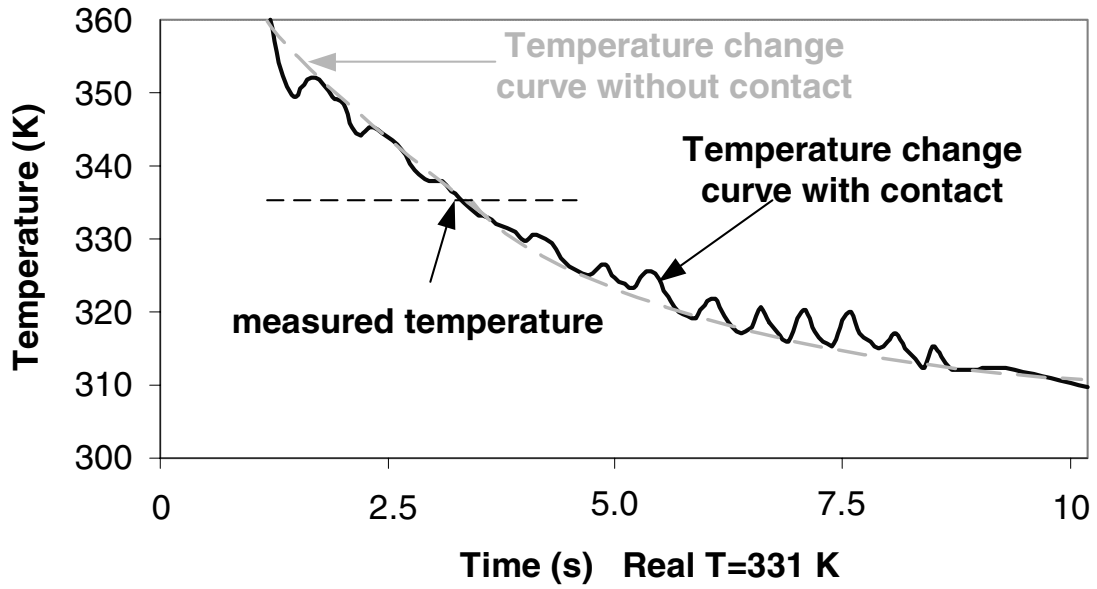
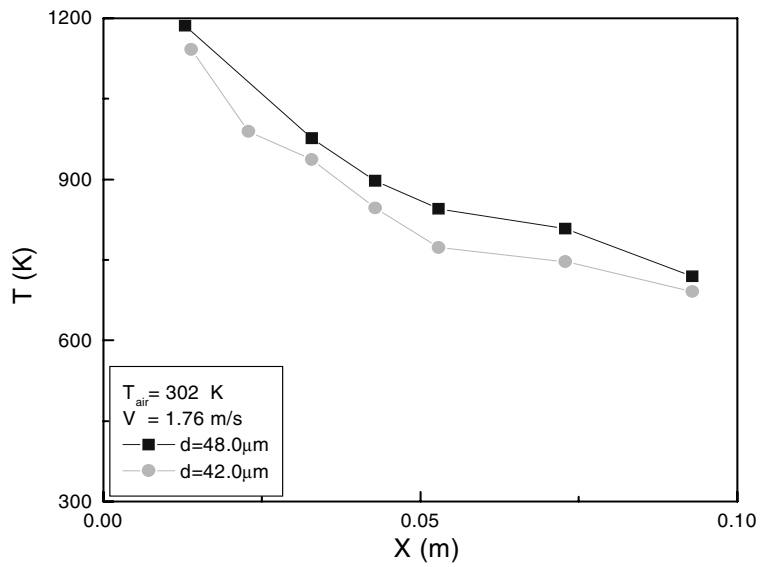
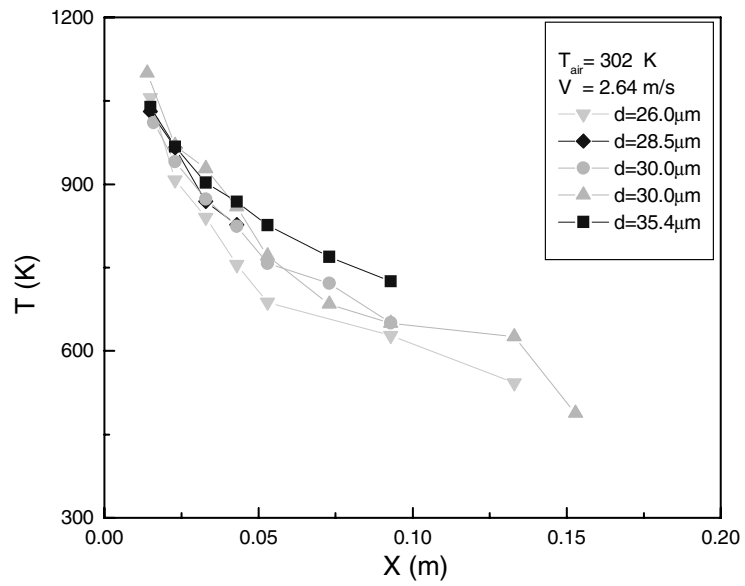


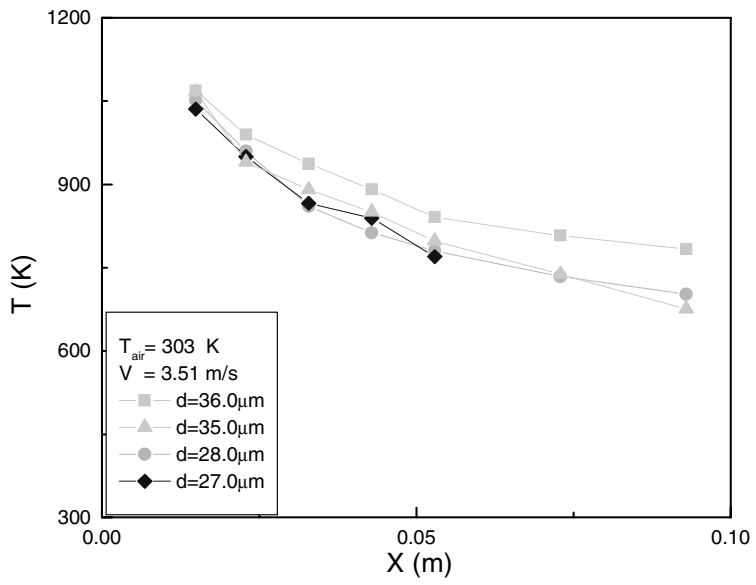
Figure 6. Transient temperature profile with repeated contacts. The actual temperature was 331 K.



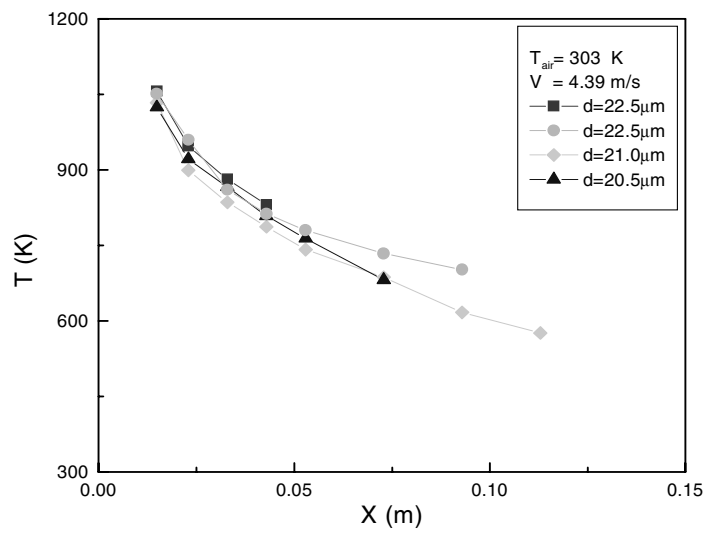
(a)



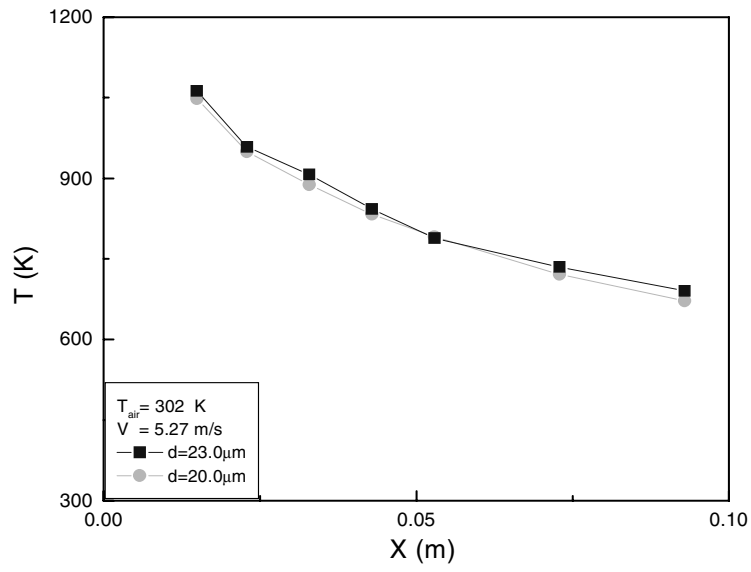
(b)



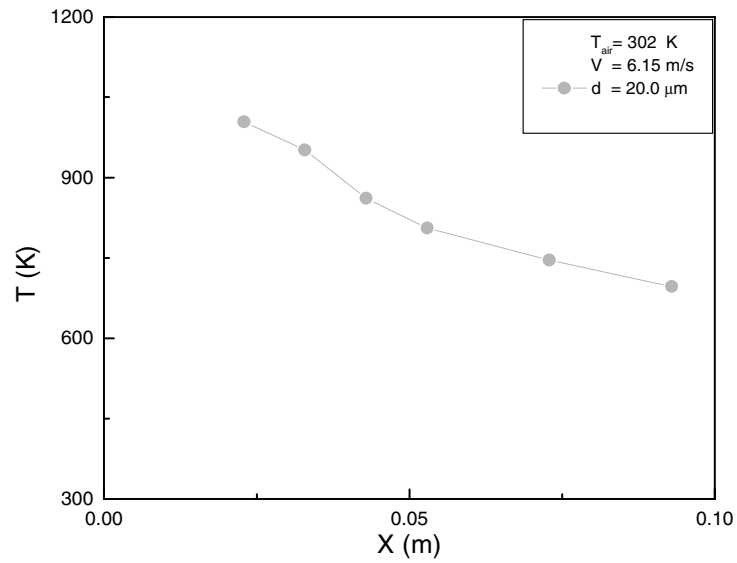
(c)



(d)



(e)



(f)

Figure 7. Temperature profiles under different drawing speeds and fiber diameters.

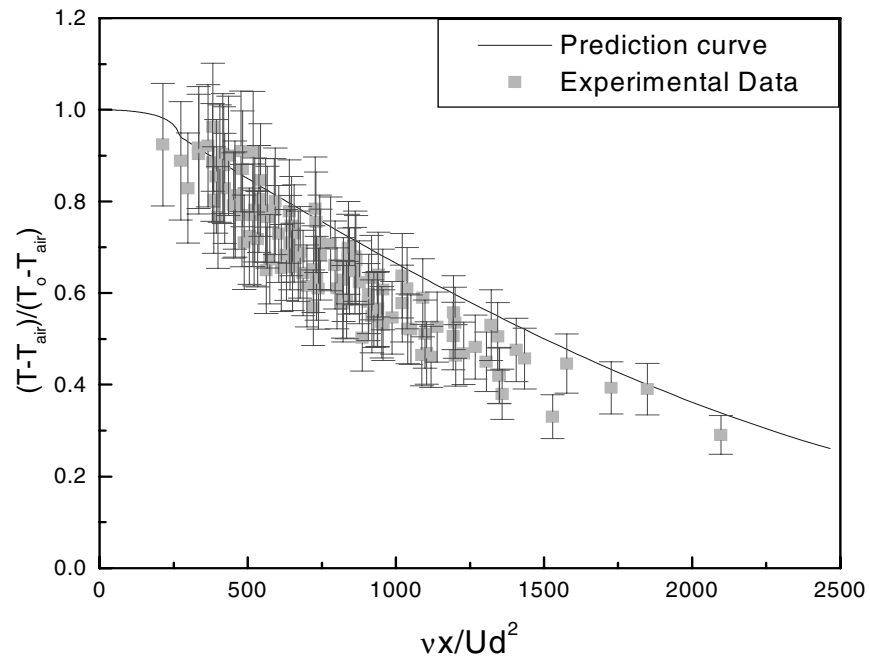


Figure 8. Comparison of our data to the integral-method prediction based on references [1,12]. Uncertainty bars are shown for each data point.

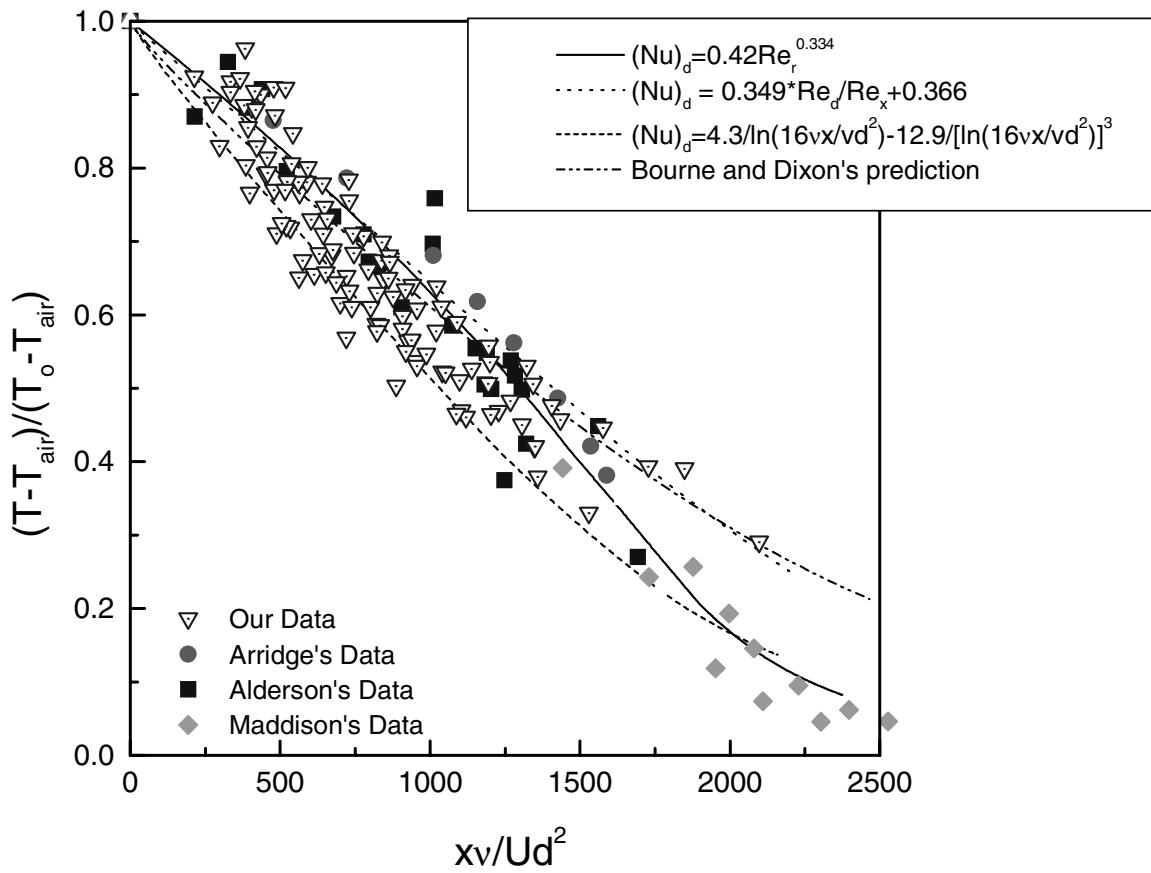


Figure 9. Comparison of past and present experimental data and predictions.